Letter

J/ψ photoproduction in Pb-Pb peripheral collisions at $\sqrt{s_{NN}} = 5$ TeV

R. Aaij *et al.**
(LHCb Collaboration)

(Received 9 August 2021; accepted 14 February 2022; published 3 March 2022)

The photoproduction of J/ψ mesons at low transverse momentum is studied in peripheral lead-lead collisions collected by the LHCb Collaboration at a center-of-mass energy per nucleon pair of 5 TeV, corresponding to an integrated luminosity of 210 μb^{-1}. The J/ψ candidates are reconstructed through the prompt decay into two muons of opposite charge in the rapidity region of $2.0 < y < 4.5$. The results significantly improve previous measurements and are compared to the latest theoretical prediction.

DOI: 10.1103/PhysRevC.105.L032201

One of the main open subjects in ultrarelativistic heavy-ion physics is the study of the quark-gluon plasma (QGP), an exotic state of hadronic matter predicted by quantum chromodynamics (QCD). Quantitative predictions of QGP properties are obtained from lattice computations [1]. Experimentally, one of the signatures of the QGP formation inside heavy-nuclei collisions is the suppression of heavy quarkonia production, such as the J/ψ particle [2]. The suppression is expected to depend on both the temperature of the medium and the binding energy of the state [3]. Cold nuclear matter effects [4] seem to influence the measurements in nuclei collisions. These effects must be understood prior to providing a sound interpretation in the QGP framework of the hadronically produced (through the interaction of two partons) quarkonia suppression observed at the BNL Relativistic Heavy Ion Collider (RHIC) and the CERN Large Hadron Collider (LHC) [5–10].

The ALICE [11] and STAR [12] Collaborations measured an excess with respect to expectations from purely hadronic production of J/ψ mesons at very low p_{T} (below 300 MeV/c), where p_{T} is the component of the J/ψ momentum transverse to the beam, in hadronic lead-lead (Pb-Pb) collisions at the center-of-mass energy per nucleon pair $\sqrt{s_{NN}} = 2.76$ TeV and gold-gold (uranium-uranium) collisions at $\sqrt{s_{NN}} = 200$ GeV (193 GeV). It was posited that this excess is due to photoproduced J/ψ mesons, caused by the coherent interaction of the large electromagnetic fields generated by the projectile with the target nucleus [13]. These types of interactions were primarily expected to only occur in ultraperipheral collisions (UPCs) [14], in which the impact parameter, b, is larger than the sum of the radii R_a and R_b of the two colliding nuclei, hence without nuclear breakup of the target or the projectile.

In hadronic collisions, the nucleus breaks up, so no coherent production was expected. A precise measurement of the postulated coherent J/ψ production in hadronic collisions would shed light on the coherence of the interaction and on the profile of the photon flux in peripheral Pb-Pb collisions [15–17].

In this Letter, a measurement of prompt J/ψ production at very-low p_{T} in Pb-Pb collisions at a center-of-mass energy per nucleon pair $\sqrt{s_{NN}} = 5\,TeV$ is reported. For the first time at the LHC, the production yield is measured versus p_{T} and rapidity, y. The data were recorded by the LHCb detector in 2018 and correspond to an integrated luminosity of about 210 μb^{-1}.

The LHCb detector [18,19] is a single-arm forward spectrometer covering the pseudorapidity range $2 < \eta < 5$, designed for the study of particles containing b or c quarks. The detector includes a high-precision tracking system consisting of a silicon-strip vertex detector surrounding the Pb-Pb interaction region [20], a large-area silicon-strip detector located upstream of a dipole magnet with a bending power of about 4 T m, and three stations of silicon-strip detectors and straw drift tubes [21] placed downstream of the magnet. The tracking system provides a measurement of the momentum of charged particles with a relative uncertainty that varies from 0.5% at low momentum to 1.0% at 200 GeV/c. The minimum distance of a track to a primary Pb-Pb collision vertex (PV), the impact parameter (IP), is measured with a resolution of $(15 + 29/p_{\mathrm{T}})$ μm, where p_{T} is the component of the momentum transverse to the beam, in GeV/c. Different types of charged hadrons are distinguished using information from two ring-imaging Cherenkov detectors [22]. Photons, electrons, and hadrons are identified by a calorimeter system consisting of scintillating-pad and preshower detectors, an electromagnetic, and a hadronic calorimeter. Muons are identified by a system composed of alternating layers of iron and multiwire proportional chambers [23].

*Full author list given at the end of the article.

The trigger consists of a hardware stage, using information from the calorimeter and muon systems, followed by a software stage, which applies selections on the fully reconstructed event.

At the hardware trigger stage, events are required to have a muon with high p_{T} or a hadron, photon, or electron with high transverse energy in the calorimeters. Two samples are selected for this analysis, a signal sample and a sample of minimum bias events used to normalize through the total number of inelastic events. They have different trigger strategies. Signal events are selected if the number of clusters in the VErtex LOcator (VELO), N_{c}, is $6000 < N_{\mathrm{c}} < 10000$ or if $N_{\mathrm{c}} < 6000$ and two muons with $p_{\mathrm{T}} > 400$ MeV/c are reconstructed.

The hardware trigger for the minimum bias (MB) events requires a minimum energy deposit in one of the subdetectors (VELO, calorimeters, muon chambers), and only events with $N_{\mathrm{c}} < 10\,000$ are kept. To improve the signal purity, events passing the software trigger are selected if the muon candidates have a $p_{\mathrm{T}} > 700$ MeV/c, the particles are consistent with originating from a primary Pb-Pb collision vertex (PV) and are identified as muons. The prompt J/ψ candidates, which include feed-down from excited charmonium states originating from b-hadron decays, are separated from the nonprompt candidates using the requirement $t_z < 0.3$ ps, where t_z is the pseudodecay time defined as $(z_{J/\psi} - z_{\mathrm{PV}})m_{J/\psi}/p_z$. Here, $(z_{J/\psi} - z_{\mathrm{PV}})$ and p_z are the distances between the J/ψ candidate decay vertex and the PV, and the candidate momentum along the beam axis, respectively, and $m_{J/\psi}$ is the known J/ψ mass [24].

During data taking, neon (Ne) gas was injected into the beam pipe near the interaction point using LHCb's SMOG (System to Measure the Overlap integral with Gas) [25] to record fixed-target collisions simultaneously with the Pb-Pb collisions. These fixed-target PbNe collisions are rejected by placing requirements on the position of the PV. In order to remove potential contamination from UPCs, which may bias the measurement especially for very low event activity, a minimal energy deposit in the electromagnetic calorimeter (ECAL) is also required ($E_{\mathrm{tot}} > 585$ GeV).

The Pb-Pb sample is divided into intervals of N_{c} which correspond to different numbers of participating nucleons, N_{part}. This quantity is related to the centrality, defined as the percentile of the total inelastic hadronic Pb-Pb cross section as a function of the released collision energy, which can be approximated by the total energy deposit in ECAL (E_{tot}). The more central is the collision, the larger E_{tot} is and the larger N_{part} is. The percentiles are determined using the Glauber Monte Carlo (GMC) model [26,27]. The model is used to perform a binned fit to the E_{tot} distribution of the MB data sample, collected with the same detector conditions as the signal sample. The quantity N_{part} is estimated for each collision and the mean value, $\langle N_{\mathrm{part}}\rangle$, is derived from events within a given N_c range. Results for each N_c interval are summarized in Table I. The distribution of N_{part} in the three N_c intervals is shown in Fig. 1. More details on the centrality determination in LHCb can be found in Ref. [28] and in the Supplemental Material [29].

TABLE I. Average number of participant nucleons, $\langle N_{\mathrm{part}}\rangle$, along with the corresponding standard deviation of the N_{part} distribution, σ_{part}, for each of the selected N_c intervals.

N_c	$\langle N_{\mathrm{part}}\rangle$	σ_{part}
1000–4000	10.6	2.9
4000–6000	15.7	4.1
6000–10000	27.8	7.2
1000–10000	19.7	9.2

In this Letter, the J/ψ photoproduction differential yield is measured, defined as

$$\frac{dY^i_{J/\psi}}{dy} = \frac{N^i_{J/\psi}}{\mathcal{B}\, N^i_{\mathrm{MB}}\, \varepsilon^i_{\mathrm{tot}}\, \Delta y}, \tag{1}$$

$$\frac{d^2Y^i_{J/\psi}}{dp_{\mathrm{T}}dy} = \frac{dY^i_{J/\psi}}{dy}\frac{1}{\Delta p_{\mathrm{T}}}, \tag{2}$$

where i indicates the N_c range, $N^i_{J/\psi}$ is the number of photoproduced J/ψ meson candidates reconstructed through the $J/\psi \to \mu^+\mu^-$ decay channel in the (p_{T}, y) interval of width $(\Delta p_{\mathrm{T}}, \Delta y)$, $\mathcal{B} = (5.961 \pm 0.033)\%$ [24] is the branching fraction of the decay $J/\psi \to \mu^+\mu^-$, N^i_{MB} is the total number of MB events, and $\varepsilon^i_{\mathrm{tot}}$ is the efficiency to reconstruct and select the J/ψ candidates. The dimuon invariant mass, $m(\mu^+\mu^-)$, of the selected candidates is shown in Fig. 2 for a representative centrality interval for J/ψ candidates with $p_{\mathrm{T}} < 15.0$ GeV/c and $2.0 < y < 4.5$. An unbinned fit of these candidates is performed using a Crystal Ball (CB) function for the signal and a first-order polynomial for the background.

Photoproduced J/ψ mesons and hadronically produced J/ψ mesons are then disentangled through an unbinned maximum likelihood fit to the dimuon p_{T} spectrum. The fit is performed after subtracting correlated background, i.e., arising from $\gamma\gamma \to \mu^+\mu^-$ or the Drell-Yan process, and combinatorial background from uncorrelated muon pairs which is the dominant source, using the *sPlot* method [30] with

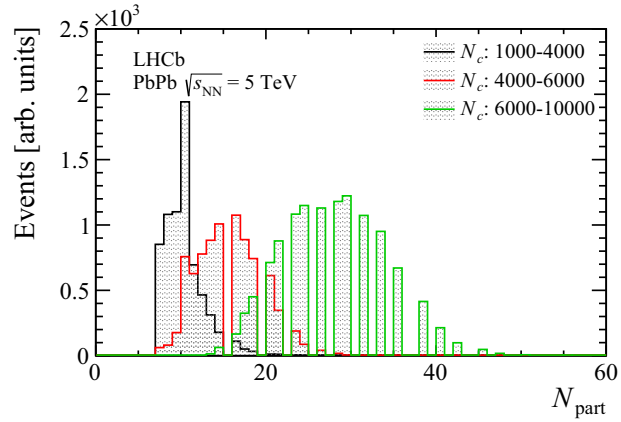

FIG. 1. Distribution of N_{part} in the three N_c intervals of the minimum bias events defined in Table I.

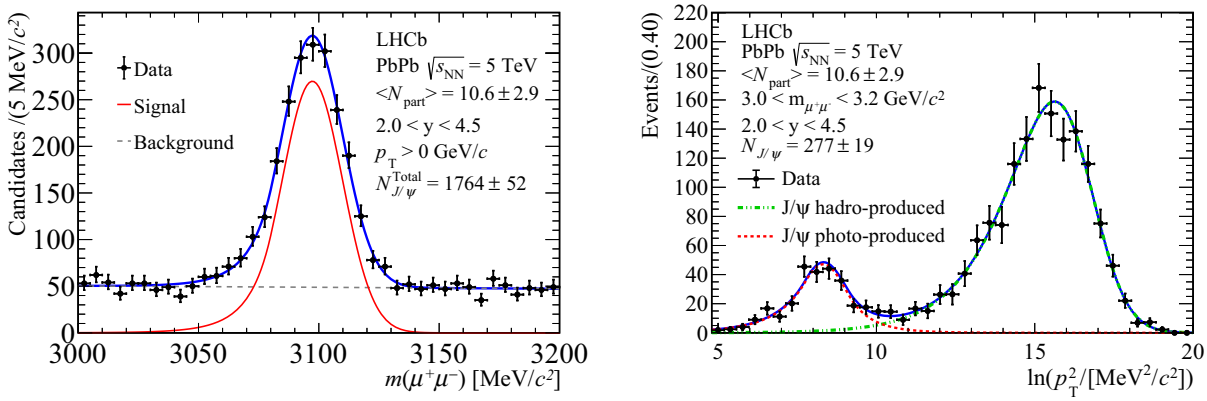

FIG. 2. Left: Invariant mass distribution of J/ψ candidates with $\langle N_{\rm part}\rangle = 10.6 \pm 2.9$, for $p_{\rm T} < 15.0$ GeV/c and $2.0 < y < 4.5$. Right: Distribution of $\ln(p_{\rm T}^2)$ of the J/ψ candidates for $\langle N_{\rm part}\rangle = 10.6 \pm 2.9$ after background subtraction. The projections of the fit to disentangle the coherently photoproduced and hadronically produced J/ψ mesons are overlaid.

$m(\mu^+\mu^-)$ as discriminating variable. To cross-check the validity of the *sPlot* method, the kinematic distributions ($p_{\rm T}$, y, N_c) of the estimated background are compared to the same (normalized) distributions in two invariant mass ranges below and above the resonance peak. A very good agreement is found. The empirical fit model comprises a double-sided Crystal Ball function [31] expressed in $\ln(p_{\rm T}^2)$ for the photoproduction contribution and a function for the hadronic component that typically has a larger $p_{\rm T}$,

$$f(p_{\rm T}) = \frac{p_{\rm T}^{n_1}}{\left[1 + \left(\frac{p_{\rm T}}{p_0}\right)^{n_2}\right]^{n_3}}, \tag{3}$$

where n_1, n_2, n_3, and p_0 are parameters free to vary in the fit. The projections of the fits in the centrality interval $\langle N_{\rm part}\rangle = 10.6 \pm 2.9$ are shown in Fig. 2, overlaid on the data distributions. A good description of the data is observed in all centrality intervals. The photoproduced J/ψ candidates are visible in the range $0 < p_{\rm T} < 250$ MeV/c. The $p_{\rm T}$ distribution of the photoproduced J/ψ candidates does not rise towards vanishing $p_{\rm T}$ due to the interference caused by the negative parity of the photon as explained in Ref. [17].

Simulation is required to model the effects of the detector acceptance and of the selection requirements on the signal. The Pb-Pb collisions are generated using EPOS [32] and the hard process is generated with PYTHIA [33] with a specific LHCb configuration [34].

An additional signal sample where the J/ψ is transversely polarised was produced using the STARLIGHT [35] generator to study the acceptance assuming the coherent photoproduction scenario. The interactions of the generated particles with the detector, and its response, are implemented using the GEANT4 toolkit [36] as described in Ref. [37]. The total efficiency is determined independently in each interval of centrality, and it includes the effects of the geometrical acceptance ($\epsilon_{\rm acc}$), the trigger efficiency ($\epsilon_{\rm trigger}$), the reconstruction and selection efficiency ($\epsilon_{\rm rec\&sel}$), and the efficiency of the particle identification (PID) criteria ($\epsilon_{\rm PID}$). The acceptance is determined using the STARLIGHT sample in the kinematic range of the analysis. The efficiency $\epsilon_{\rm rec\&sel}$ is estimated using simulation and data calibration techniques. The main component of the reconstruction inefficiency is due to the tracking algorithms, as the performance is affected by the high occupancy in Pb-Pb collisions. The relative reconstruction efficiency between data and simulation is evaluated using two D^0 meson decay channels ($D^0 \to K^-\pi^+$ and $D^0 \to K^-\pi^+\pi^-\pi^+$). The yields are evaluated in Pb-Pb data and simulation and the difference of their ratio to unity is encoded in a factor $k(N_c)$. This factor depends on the event multiplicity with k ranging from 0.97 to 0.91 with increasing N_c, assuming $k(N_c)$ is the same for the π and μ tracks. The latter factor is used to correct the reconstructed J/ψ candidates in simulation. An additional correction is applied to correct discrepancies between reconstructed J/ψ kinematic distributions by weighting the variables N_c, $p_{\rm T}$, and y of the J/ψ in simulation to match the data. The PID efficiency $\epsilon_{\rm PID}$ is evaluated using a tag-and-probe approach with $J/\psi \to \mu\mu$ decays reconstructed in proton-proton collisions that provide PID efficiency tables for single muons. Those efficiencies are used to perform a two-dimensional (p_T, N_c) extrapolation, using first- and second-order polynomial functions, to estimate the decrease of the efficiencies for higher multiplicities seen in Pb-Pb collisions. No extrapolation is performed based on the rapidity as no correlation is seen between N_c and y.

Several sources of systematic uncertainties are considered. The uncertainty associated with the fit model used to evaluate the signal yields is determined by testing alternative fit functions. The $p_{\rm T}$ of the hadronically produced J/ψ candidates is modeled by a Tsallis function [38]. The background shape is also modified to account for incoherent photoproduced J/ψ, defined as the interaction between one photon and a single nucleon implying the destruction of the nucleus. This contribution typically produces J/ψ mesons at higher $p_{\rm T}$ than the coherent photoproduction source. Therefore, another double CB function is added to model this potential contribution. The incoherent contribution shares the shape parameters of the coherent contribution with the mean $p_{\rm T}$ and width shifted according to the differences obtained in the STARLIGHT simulations. By computing the difference to the reference fit, a total uncertainty of about 1.3% averaged over all centrality intervals is obtained.

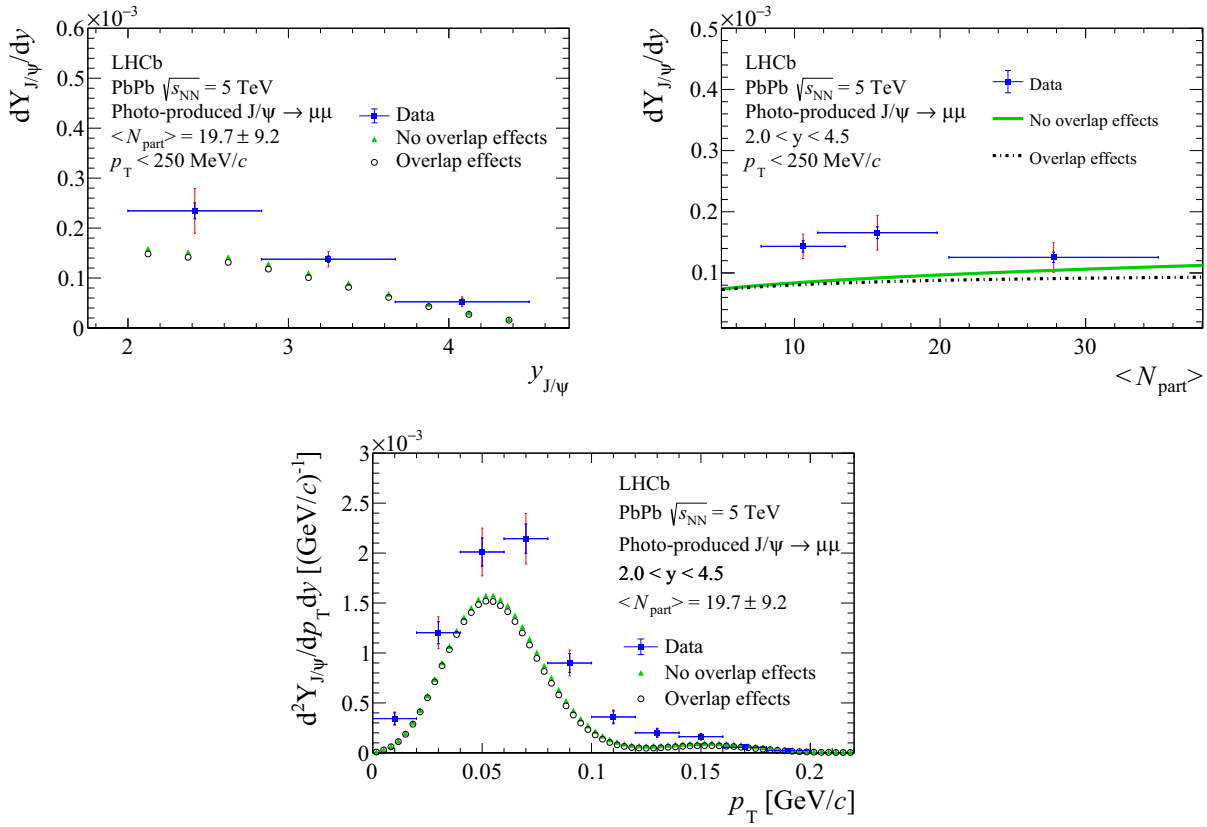

FIG. 3. Top left: Differential yields of photoproduced J/ψ candidates as a function of rapidity and (top right) $\langle N_{\rm part}\rangle$. Bottom: Double differential yields as a function of $p_{\rm T}$. The vertical inner blue bars represent the statistical uncertainty and the outer red bars the total uncertainty. The horizontal bars in the $\langle N_{\rm part}\rangle$ results correspond to the standard deviation of the $N_{\rm part}$ distribution of the MB events. The yields are compared to the prediction from Ref. [17,39] that take (black) or do not take (green) into account the effect from the overlap region of the collision.

The systematic uncertainty associated with the evaluation of the efficiencies is divided into uncertainties due to the $\epsilon_{\rm rec\&sel}$, $\epsilon_{\rm PID}$, and $\epsilon_{\rm trigger}$ efficiencies. Three systematic effects are considered for the measurement of $\epsilon_{\rm rec\&sel}$: The uncertainty on the weighting procedure, the uncertainty associated with the evaluation of the factor k, and the correlation between the variables $p_{\rm T}$ and y. The uncertainty on the weighting procedure is estimated by comparing $p_{\rm T}$, y, and N_c of the weighted distributions of the J/ψ mesons in simulation with those in data after background subtraction. The difference between the two leads to a global uncertainty of 2%. The uncertainty on the factor k is evaluated by varying its value within its uncertainty and propagating it to the tracking efficiency. An uncertainty from 2.9% to 7.4% is found depending on the considered multiplicity interval. The uncertainty on the correlation between the variables $p_{\rm T}$ and y is estimated to be 1% using calibration samples from proton-proton collisions.

The uncertainty coming from the muon PID efficiency tables is evaluated with a smearing technique. The J/ψ PID efficiency is computed using efficiency PID tables with the values in each interval varied within their uncertainty. This procedure is repeated several times and the largest difference is taken as systematic uncertainty; the effect is smaller than 1% and considered negligible compared to the uncertainty given by the difference of the two functions used for the extrapolation.

The uncertainty on $\epsilon_{\rm trigger}$ is estimated by comparing the trigger efficiency measurement with another method based on data. The method consists of evaluating the efficiency using a sample selected by the same trigger algorithms but independent from those used in the selection of the signal. The difference of 3% between the two methods is taken as systematic uncertainty on the trigger efficiency. The total systematic uncertainties are obtained by summing in quadrature the different sources of uncertainties.

The differential J/ψ photoproduction yields, Eq. (1), as a function of the rapidity for $\langle N_{\rm part}\rangle = 19.7 \pm 9.2$ and as a function of $\langle N_{\rm part}\rangle$ are shown in Fig. 3 (top). The double-differential J/ψ photoproduction yields, Eq. (2), as a function of the transverse momentum are as well shown in Fig. 3 (bottom). The mean $p_{\rm T}$ of the coherent J/ψ is found to be $\langle p_T\rangle = 64.9 \pm 2.4$ MeV/c. The results are compared to the theoretical prediction [17,39] and detailed results are presented in the Supplemental Material [29]. The model assumes two scenarios in which the coherence of the J/ψ production is (overlap effect) or is not (no overlap effect) affected by interactions with the overlap region of the two colliding nuclei. Little difference is observed between the two theory scenarios. The divergence is important in more central collisions due to the increase of the photon flux with a decrease of the impact parameter. In the overlapping scenario, this effect is balanced by excluding the overlapping region from the interaction.

The measured yield of the coherent J/ψ production is higher at low rapidity than at high rapidity and it is consistent with being constant with respect to $\langle N_{\rm part}\rangle$ for the region considered in the analysis.

In summary, the yield of coherently photoproduced prompt J/ψ mesons at very low $p_{\rm T}$ in peripheral Pb-Pb collisions collected at $\sqrt{s_{NN}} = 5$ TeV is measured with the LHCb experiment. The yields are studied as a function of rapidity and transverse momentum of the J/ψ meson in intervals of the number of participant nucleons $\langle N_{\rm part}\rangle$. These results are the most precise to date, and support the hypothesis of coherent J/ψ photoproduction in peripheral hadronic collisions suggested by the other experiments [11,12]. The shape of the results is qualitatively described by the theoretical prediction [17,39], although a normalization discrepancy is observed which could hide a possible additional contribution.

We express our gratitude to our colleagues in the CERN accelerator departments for the excellent performance of the LHC. We thank the technical and administrative staff at the LHCb institutes. We acknowledge support from CERN and from the following national agencies: CAPES, CNPq, FAPERJ, and FINEP(Brazil); MOST and NSFC (China); CNRS/IN2P3 (France); BMBF, DFG, and MPG (Germany); INFN (Italy); NWO (Netherlands); MNiSW and NCN (Poland); MEN/IFA (Romania); MSHE (Russia); MICINN (Spain); SNSF and SER (Switzerland); NASU (Ukraine); STFC (United Kingdom); DOE NP and NSF (USA). We acknowledge the computing resources that are provided by CERN, IN2P3 (France), KIT and DESY (Germany), INFN (Italy), SURF (Netherlands), PIC (Spain), GridPP (United Kingdom), RRCKI and Yandex LLC (Russia), CSCS (Switzerland), IFIN-HH (Romania), CBPF (Brazil), PL-GRID (Poland), and NERSC (USA). We are indebted to the communities behind the multiple open-source software packages on which we depend. Individual groups or members have received support from ARC and ARDC (Australia); AvH Foundation (Germany); EPLANET, Marie Skłodowska-Curie Actions, and ERC (European Union); A*MIDEX, ANR, IPhU and Labex P2IO, and Région Auvergne-Rhône-Alpes (France); Key Research Program of Frontier Sciences of CAS, CAS PIFI, CAS CCEPP, Fundamental Research Funds for the Central Universities, and Sci. & Tech. Program of Guangzhou (China); RFBR, RSF, and Yandex LLC (Russia); GVA, XuntaGal, and GENCAT (Spain); the Leverhulme Trust, the Royal Society, and UKRI (United Kingdom).

[1] Y. Aoki *et al.*, The order of the quantum chromodynamics transition predicted by the standard model of particle physics, Nature (London) **443**, 675 (2006).
[2] T. Matsui and H. Satz, J/ψ suppression by quark-gluon plasma formation, Phys. Lett. B **178**, 416 (1986).
[3] L. Yan, P. Zhuang, and N. Xu, Competition between J/ψ Suppression and Regeneration in Quark-Gluon Plasma, Phys. Rev. Lett. **97**, 232301 (2006).
[4] E. G. Ferreiro, F. Fleuret, J. P. Lansberg, and A. Rakotozafindrabe, Cold nuclear matter effects on J/ψ production: Intrinsic and extrinsic transverse momentum effects, Phys. Lett. B **680**, 50 (2009).
[5] S. Acharya *et al.* (ALICE Collaboration), Studies of J/ψ production at forward rapidity in Pb-Pb collisions at $\sqrt{s_{\rm NN}} =$ 5.02 TeV, J. High Energy Phys. 02 (2020) 041.
[6] V. Khachatryan *et al.* (CMS Collaboration), Suppression of $\Upsilon(1S)$, $\Upsilon(2S)$ and $\Upsilon(3S)$ quarkonium states in PbPb collisions at $\sqrt{s_{NN}} = 2.76$ TeV, Phys. Lett. B **770**, 357 (2017).
[7] S. Chatrchyan *et al.* (CMS Collaboration), Indications of Suppression of Excited Υ States in Pb-Pb Collisions at $\sqrt{s_{NN}} =$ 2.76 TeV, Phys. Rev. Lett. **107**, 052302 (2011).
[8] M. Aaboud *et al.* (ATLAS Collaboration), Measurement of quarkonium production in proton–lead and proton–proton collisions at 5.02 TeV with the ATLAS detector, Eur. Phys. J. C **78**, 171 (2018).
[9] A. M. Sirunyan *et al.* (CMS Collaboration), Suppression of Excited Υ States Relative to the Ground State in Pb-Pb Collisions at $\sqrt{s_{NN}} = 5.02$ TeV, Phys. Rev. Lett. **120**, 142301 (2018).
[10] B. B. Abelev *et al.* (ALICE Collaboration), Production of inclusive Υ(1S) and Υ(2S) in p-Pb collisions at $\sqrt{s_{NN}} = 5.02$ TeV, Phys. Lett. B **740**, 105 (2015)
[11] J. Adam *et al.* (ALICE Collaboration), Measurement of an Excess in the Yield of J/ψ at Very Low $p_{\rm T}$ in Pb-Pb Collisions at $\sqrt{s_{NN}} = 2.76$ TeV, Phys. Rev. Lett. **116**, 222301 (2016).
[12] J. Adam *et al.* (STAR Collaboration), Observation of Excess J/ψ Yield at Very Low Transverse Momenta in Au + Au Collisions at $\sqrt{s_{NN}} = 200$ GeV and U + U Collisions at $\sqrt{s_{NN}} =$ 193 GeV, Phys. Rev. Lett. **123**, 132302 (2019).
[13] E. J. Williams, Nature of the high energy particles of penetrating radiation and status of ionization and radiation formulae, Phys. Rev. **45**, 729 (1934).
[14] A. Baltz *et al.*, The physics of ultraperipheral collisions at the LHC, Phys. Rep. **458**, 1 (2008).
[15] M. B. G. Ducati and S. Martins, Heavy meson photoproduction in peripheral *AA* collisions, Phys. Rev. D **97**, 116013 (2018).
[16] J. Cepila, and J. G. Contreras, and M. Krelina, Coherent and incoherent J/ψ photonuclear production in an energy-dependent hot-spot model, Phys. Rev. C **97**, 024901 (2018).
[17] W. Zha *et al.*, Coherent J/ψ photoproduction in hadronic heavy-ion collisions, Phys. Rev. C **97**, 044910 (2018).
[18] A. A. Alves Jr. *et al.* (LHCb Collaboration), The LHCb detector at the LHC, J. Instrum. **3**, S08005 (2008).
[19] R. Aaij *et al.* (LHCb Collaboration), LHCb detector performance, Int. J. Mod. Phys. A **30**, 1530022 (2015).
[20] R. Aaij *et al.* (LHCb Collaboration), Performance of the LHCb Vertex Locator, J. Instrum. **9**, P09007 (2014).
[21] Ph. d'Argent, and others, Improved performance of the LHCb Outer Tracker in LHC Run 2, J. Instrum. **12**, P11016 (2017).
[22] M. Adinolfi, and others, Performance of the LHCb RICH detector at the LHC, Eur. Phys. J. C **73**, 2431 (2013).
[23] A. A. Alves, Jr., and others, Performance of the LHCb muon system, J. Instrum. **8**, P02022 (2013).
[24] P. A. Zyla *et al.*, (Particle Data Group), Review of Particle Physics, Prog. Theor. Exp. Phys. **2020**, 083C01 (2020).
[25] R. Aaij *et al.* (LHCb Collaboration), Precision luminosity measurements at LHCb, J. Instrum. **9**, P12005 (2014).

[26] C. Loizides, J. Kamin, and D. d'Enterria, Improved Monte Carlo Glauber predictions at present and future nuclear colliders, Phys. Rev. C **97**, 054910 (2018).
[27] B. Abelev *et al.* (ALICE Collaboration), Centrality determination of Pb-Pb collisions at $\sqrt{s_{NN}} = 2.76$ TeV with ALICE, Phys. Rev. C **88**, 044909 (2013).
[28] R. Aaij *et al.*, Centrality determination in heavy-ion collisions with the LHCb detector, LHCb-DP-2021-001 (unpublished).
[29] See Supplemental Material at http://link.aps.org/supplemental/10.1103/PhysRevC.105.L032201 for additional information on the centrality measurement and detailed results of the photoproduced J/ψ mesons measurement.
[30] M. Pivk and F. R. Le Diberder, sPlot: A statistical tool to unfold data distributions, Nucl. Instrum. Methods A **555**, 356 (2005).
[31] T. Skwarnicki, A study of the radiative cascade transitions between the Upsilon-prime and Upsilon resonances, Ph.D. thesis, Institute of Nuclear Physics, Krakow, 1986, DESY-F31-86-02 (unpublished).
[32] T. Pierog, I. Karpenko, J.M. Katzy, E. Yatsenko, and K. Werner, EPOS LHC: Test of collective hadronization with data measured at the CERN Large Hadron Collider, Phys. Rev. C **92**, 034906 (2015).
[33] T. Sjöstrand, S. Mrenna, and P. Skands, A brief introduction to PYTHIA 8.1, Comput. Phys. Commun. **178**, 852 (2008); PYTHIA 6.4 physics and manual, J. High Energy Phys. 05 (2006) 026.
[34] I. Belyaev *et al.*, Handling of the generation of primary events in Gauss, the LHCb simulation framework, J. Phys.: Conf. Ser. **331**, 032047 (2011).
[35] S. Klein *et al.*, STAR light: A Monte Carlo simulation program for ultra-peripheral collisions of relativistic ions, Comput. Phys. Commun. **212**, 258 (2017).
[36] J. Allison *et al.* (Geant4 Collaboration), Geant4 developments and applications, IEEE Trans. Nucl. Sci. **53**, 270 (2006); S. Agostinelli *et al.* (Geant4 Collaboration), Geant4: A simulation toolkit, Nucl. Instrum. Methods Phys. A **506**, 250 (2003)..
[37] M. Clemencic *et al.*, The LHCb simulation application, Gauss: Design, evolution and experience, J. Phys.: Conf. Ser. **331**, 032023 (2011).
[38] C. Tsallis, Nonextensive statistics: theoretical, experimental and computational evidences and connections, Braz. J. Phys. **29**, 1 (1999).
[39] W. Zha, L. Ruan, Z. Tang, Z. Xu, and S. Yang, Double-slit experiment at Fermi scale: Coherent photoproduction in heavy-ion collisions, Phys. Rev. C **99**, 061901(R) (2019).

R. Aaij,[32] C. Abellán Beteta,[50] T. Ackernley,[60] B. Adeva,[46] M. Adinolfi,[54] H. Afsharnia,[9] C. A. Aidala,[85] S. Aiola,[25] Z. Ajaltouni,[9] S. Akar,[65] J. Albrecht,[15] F. Alessio,[48] M. Alexander,[59] A. Alfonso Albero,[45] Z. Aliouche,[62] G. Alkhazov,[38] P. Alvarez Cartelle,[55] S. Amato,[2] Y. Amhis,[11] L. An,[48] L. Anderlini,[22] A. Andreianov,[38] M. Andreotti,[21] F. Archilli,[17] A. Artamonov,[44] M. Artuso,[68] K. Arzymatov,[42] E. Aslanides,[10] M. Atzeni,[50] B. Audurier,[12] S. Bachmann,[17] M. Bachmayer,[49] J. J. Back,[56] P. Baladron Rodriguez,[46] V. Balagura,[12] W. Baldini,[21] J. Baptista Leite,[1] R. J. Barlow,[62] S. Barsuk,[11] W. Barter,[61] M. Bartolini,[24,a] F. Baryshnikov,[82] J. M. Basels,[14] G. Bassi,[29] B. Batsukh,[68] A. Battig,[15] A. Bay,[49] M. Becker,[15] F. Bedeschi,[29] I. Bediaga,[1] A. Beiter,[68] V. Belavin,[42] S. Belin,[27] V. Bellee,[49] K. Belous,[44] I. Belov,[40] I. Belyaev,[41] G. Bencivenni,[23] E. Ben-Haim,[13] A. Berezhnoy,[40] R. Bernet,[50] D. Berninghoff,[17] H. C. Bernstein,[68] C. Bertella,[48] A. Bertolin,[28] C. Betancourt,[50] F. Betti,[48] Ia. Bezshyiko,[50] S. Bhasin,[54] J. Bhom,[35] L. Bian,[73] M. S. Bieker,[15] S. Bifani,[53] P. Billoir,[13] M. Birch,[61] F. C. R. Bishop,[55] A. Bitadze,[62] A. Bizzeti,[22,b] M. Bjørn,[63] M. P. Blago,[48] T. Blake,[56] F. Blanc,[49] S. Blusk,[68] D. Bobulska,[59] J. A. Boelhauve,[15] O. Boente Garcia,[46] T. Boettcher,[65] A. Boldyrev,[81] A. Bondar,[43] N. Bondar,[38,48] S. Borghi,[62] M. Borisyak,[42] M. Borsato,[17] J. T. Borsuk,[35] S. A. Bouchiba,[49] T. J. V. Bowcock,[60] A. Boyer,[48] C. Bozzi,[21] M. J. Bradley,[61] S. Braun,[66] A. Brea Rodriguez,[46] M. Brodski,[48] J. Brodzicka,[35] A. Brossa Gonzalo,[56] D. Brundu,[27] A. Buonaura,[50] C. Burr,[48] A. Bursche,[72] A. Butkevich,[39] J. S. Butter,[32] J. Buytaert,[48] W. Byczynski,[48] S. Cadeddu,[27] H. Cai,[73] R. Calabrese,[21,c] L. Calefice,[15,13] L. Calero Diaz,[23] S. Cali,[23] R. Calladine,[53] M. Calvi,[26,d] M. Calvo Gomez,[84] P. Camargo Magalhaes,[54] A. Camboni,[45,84] P. Campana,[23] A. F. Campoverde Quezada,[6] S. Capelli,[26,d] L. Capriotti,[20,e] A. Carbone,[20,e] G. Carboni,[31] R. Cardinale,[24,a] A. Cardini,[27] I. Carli,[4] P. Carniti,[26,d] L. Carus,[14] K. Carvalho Akiba,[32] A. Casais Vidal,[46] G. Casse,[60] M. Cattaneo,[48] G. Cavallero,[48] S. Celani,[49] J. Cerasoli,[10] A. J. Chadwick,[60] M. G. Chapman,[54] M. Charles,[13] Ph. Charpentier,[48] G. Chatzikonstantinidis,[53] C. A. Chavez Barajas,[60] M. Chefdeville,[8] C. Chen,[3] S. Chen,[4] A. Chernov,[35] V. Chobanova,[46] S. Cholak,[49] M. Chrzaszcz,[35] A. Chubykin,[38] V. Chulikov,[38] P. Ciambrone,[23] M. F. Cicala,[56] X. Cid Vidal,[46] G. Ciezarek,[48] P. E. L. Clarke,[58] M. Clemencic,[48] H. V. Cliff,[55] J. Closier,[48] J. L. Cobbledick,[62] V. Coco,[48] J. A. B. Coelho,[11] J. Cogan,[10] E. Cogneras,[9] L. Cojocariu,[37] P. Collins,[48] T. Colombo,[48] L. Congedo,[19,f] A. Contu,[27] N. Cooke,[53] G. Coombs,[59] G. Corti,[48] C. M. Costa Sobral,[56] B. Couturier,[48] D. C. Craik,[64] J. Crkovská,[67] M. Cruz Torres,[1] R. Currie,[58] C. L. Da Silva,[67] E. Dall'Occo,[15] J. Dalseno,[46] C. D'Ambrosio,[48] A. Danilina,[41] P. d'Argent,[48] A. Davis,[62] O. De Aguiar Francisco,[62] K. De Bruyn,[78] S. De Capua,[62] M. De Cian,[49] J. M. De Miranda,[1] L. De Paula,[2] M. De Serio,[19,f] D. De Simone,[50] P. De Simone,[23] J. A. de Vries,[79] C. T. Dean,[67] D. Decamp,[8] L. Del Buono,[13] B. Delaney,[55] H.-P. Dembinski,[15] A. Dendek,[34] V. Denysenko,[50] D. Derkach,[81] O. Deschamps,[9] F. Desse,[11] F. Dettori,[27,g] B. Dey,[73] P. Di Nezza,[23] S. Didenko,[82] L. Dieste Maronas,[46] H. Dijkstra,[48] V. Dobishuk,[52] A. M. Donohoe,[18] F. Dordei,[27] A. C. dos Reis,[1] L. Douglas,[59] A. Dovbnya,[51] A. G. Downes,[8] K. Dreimanis,[60] M. W. Dudek,[35] L. Dufour,[48] V. Duk,[77] P. Durante,[48] J. M. Durham,[67] D. Dutta,[62] A. Dziurda,[35] A. Dzyuba,[38] S. Easo,[57] U. Egede,[69] V. Egorychev,[41] S. Eidelman,[43,h] S. Eisenhardt,[58] S. Ek-In,[49] L. Eklund,[59,i] S. Ely,[68] A. Ene,[37] E. Epple,[67] S. Escher,[14] J. Eschle,[50] S. Esen,[13] T. Evans,[48] A. Falabella,[20] J. Fan,[3] Y. Fan,[6] B. Fang,[73] S. Farry,[60] D. Fazzini,[26,d] M. Féo,[48] A. Fernandez Prieto,[46] A. D. Fernez,[66] F. Ferrari,[20,e] L. Ferreira Lopes,[49] F. Ferreira Rodrigues,[2] S. Ferreres Sole,[32] M. Ferrillo,[50] M. Ferro-Luzzi,[48] S. Filippov,[39] R. A. Fini,[19] M. Fiorini,[21,c] M. Firlej,[34] K. M. Fischer,[63] D. S. Fitzgerald,[85]

C. Fitzpatrick,[62] T. Fiutowski,[34] F. Fleuret,[12] M. Fontana,[13] F. Fontanelli,[24,a] R. Forty,[48] V. Franco Lima,[60] M. Franco Sevilla,[66] M. Frank,[48] E. Franzoso,[21] G. Frau,[17] C. Frei,[48] D. A. Friday,[59] J. Fu,[25] Q. Fuehring,[15] W. Funk,[48] E. Gabriel,[32] T. Gaintseva,[42] A. Gallas Torreira,[46] D. Galli,[20,e] S. Gambetta,[58,48] Y. Gan,[3] M. Gandelman,[2] P. Gandini,[25] Y. Gao,[5] M. Garau,[27] L. M. Garcia Martin,[56] P. Garcia Moreno,[45] J. García Pardiñas,[26,d] B. Garcia Plana,[46] F. A. Garcia Rosales,[12] L. Garrido,[45] C. Gaspar,[48] R. E. Geertsema,[32] D. Gerick,[17] L. L. Gerken,[15] E. Gersabeck,[62] M. Gersabeck,[62] T. Gershon,[56] D. Gerstel,[10] Ph. Ghez,[8] V. Gibson,[55] H. K. Giemza,[36] M. Giovannetti,[23,j] A. Gioventù,[46] P. Gironella Gironell,[45] L. Giubega,[37] C. Giugliano,[21,48,c] K. Gizdov,[58] E. L. Gkougkousis,[48] V. V. Gligorov,[13] C. Göbel,[70] E. Golobardes,[84] D. Golubkov,[41] A. Golutvin,[61,82] A. Gomes,[1,k] S. Gomez Fernandez,[45] F. Goncalves Abrantes,[63] M. Goncerz,[35] G. Gong,[3] P. Gorbounov,[41] I. V. Gorelov,[40] C. Gotti,[26] E. Govorkova,[48] J. P. Grabowski,[17] T. Grammatico,[13] L. A. Granado Cardoso,[48] E. Graugés,[45] E. Graverini,[49] G. Graziani,[22] A. Grecu,[37] L. M. Greeven,[32] P. Griffith,[21,c] L. Grillo,[62] S. Gromov,[82] B. R. Gruberg Cazon,[63] C. Gu,[3] M. Guarise,[21] P. A. Günther,[17] E. Gushchin,[39] A. Guth,[14] Y. Guz,[44] T. Gys,[48] T. Hadavizadeh,[69] G. Haefeli,[49] C. Haen,[48] J. Haimberger,[48] T. Halewood-leagas,[60] P. M. Hamilton,[66] Q. Han,[7] X. Han,[17] T. H. Hancock,[63] S. Hansmann-Menzemer,[17] N. Harnew,[63] T. Harrison,[60] C. Hasse,[48] M. Hatch,[48] J. He,[6,1] M. Hecker,[61] K. Heijhoff,[32] K. Heinicke,[15] A. M. Hennequin,[48] K. Hennessy,[60] L. Henry,[25,47] J. Heuel,[14] A. Hicheur,[2] D. Hill,[49] M. Hilton,[62] S. E. Hollitt,[15] J. Hu,[17] J. Hu,[72] W. Hu,[7] W. Huang,[6] X. Huang,[73] W. Hulsbergen,[32] R. J. Hunter,[56] M. Hushchyn,[81] D. Hutchcroft,[60] D. Hynds,[32] P. Ibis,[15] M. Idzik,[34] D. Ilin,[38] P. Ilten,[65] A. Inglessi,[38] A. Ishteev,[82] K. Ivshin,[38] R. Jacobsson,[48] S. Jakobsen,[48] E. Jans,[32] B. K. Jashal,[47] A. Jawahery,[66] V. Jevtic,[15] F. Jiang,[3] M. John,[63] D. Johnson,[48] C. R. Jones,[55] T. P. Jones,[56] B. Jost,[48] N. Jurik,[48] S. Kandybei,[51] Y. Kang,[3] M. Karacson,[48] M. Karpov,[81] F. Keizer,[48] M. Kenzie,[56] T. Ketel,[33] B. Khanji,[15] A. Kharisova,[83] S. Kholodenko,[44] T. Kirn,[14] V. S. Kirsebom,[49] O. Kitouni,[64] S. Klaver,[32] K. Klimaszewski,[36] S. Koliiev,[52] A. Kondybayeva,[82] A. Konoplyannikov,[41] P. Kopciewicz,[34] R. Kopecna,[17] P. Koppenburg,[32] M. Korolev,[40] I. Kostiuk,[32,52] O. Kot,[52] S. Kotriakhova,[21,38] P. Kravchenko,[38] L. Kravchuk,[39] R. D. Krawczyk,[48] M. Kreps,[56] F. Kress,[61] S. Kretzschmar,[14] P. Krokovny,[43,h] W. Krupa,[34] W. Krzemien,[36] W. Kucewicz,[35,m] M. Kucharczyk,[35] V. Kudryavtsev,[43,h] H. S. Kuindersma,[32,33] G. J. Kunde,[67] T. Kvaratskheliya,[41] D. Lacarrere,[48] G. Lafferty,[62] A. Lai,[27] A. Lampis,[27] D. Lancierini,[50] J. J. Lane,[62] R. Lane,[54] G. Lanfranchi,[23] C. Langenbruch,[14] J. Langer,[15] O. Lantwin,[50] T. Latham,[56] F. Lazzari,[29,n] R. Le Gac,[10] S. H. Lee,[85] R. Lefèvre,[9] A. Leflat,[40] S. Legotin,[82] O. Leroy,[10] T. Lesiak,[35] B. Leverington,[17] H. Li,[72] L. Li,[63] P. Li,[17] S. Li,[7] Y. Li,[4] Y. Li,[4] Z. Li,[68] X. Liang,[68] T. Lin,[61] R. Lindner,[48] V. Lisovskyi,[15] R. Litvinov,[27] G. Liu,[72] H. Liu,[6] S. Liu,[4] X. Liu,[3] A. Loi,[27] J. Lomba Castro,[46] I. Longstaff,[59] J. H. Lopes,[2] G. H. Lovell,[55] Y. Lu,[4] D. Lucchesi,[28,o] S. Luchuk,[39] M. Lucio Martinez,[32] V. Lukashenko,[32,52] Y. Luo,[3] A. Lupato,[62] E. Luppi,[21,c] O. Lupton,[56] A. Lusiani,[29,p] X. Lyu,[6] L. Ma,[4] R. Ma,[6] S. Maccolini,[20,e] F. Machefert,[11] F. Maciuc,[37] V. Macko,[49] P. Mackowiak,[15] S. Maddrell-Mander,[54] O. Madejczyk,[34] L. R. Madhan Mohan,[54] O. Maev,[38] A. Maevskiy,[81] D. Maisuzenko,[38] M. W. Majewski,[34] J. J. Malczewski,[35] S. Malde,[63] B. Malecki,[48] A. Malinin,[80] T. Maltsev,[43,h] H. Malygina,[17] G. Manca,[27,g] G. Mancinelli,[10] D. Manuzzi,[20,e] D. Marangotto,[25,q] J. Maratas,[9,r] J. F. Marchand,[8] U. Marconi,[20] S. Mariani,[22,s] C. Marin Benito,[48] M. Marinangeli,[49] J. Marks,[17] A. M. Marshall,[54] P. J. Marshall,[60] G. Martellotti,[30] L. Martinazzoli,[48,d] M. Martinelli,[26,d] D. Martinez Santos,[46] F. Martinez Vidal,[47] A. Massafferri,[1] M. Materok,[14] R. Matev,[48] A. Mathad,[50] Z. Mathe,[48] V. Matiunin,[41] C. Matteuzzi,[26] K. R. Mattioli,[85] A. Mauri,[32] E. Maurice,[12] J. Mauricio,[45] M. Mazurek,[48] M. McCann,[61] L. Mcconnell,[18] T. H. Mcgrath,[62] A. McNab,[62] R. McNulty,[18] J. V. Mead,[60] B. Meadows,[65] C. Meaux,[10] G. Meier,[15] N. Meinert,[76] D. Melnychuk,[36] S. Meloni,[26,d] M. Merk,[32,79] A. Merli,[25] L. Meyer Garcia,[2] M. Mikhasenko,[48] D. A. Milanes,[74] E. Millard,[56] M. Milovanovic,[48] M.-N. Minard,[8] A. Minotti,[21] L. Minzoni,[21,c] S. E. Mitchell,[58] B. Mitreska,[62] D. S. Mitzel,[48] A. Mödden,[15] R. A. Mohammed,[63] R. D. Moise,[61] T. Mombächer,[15] I. A. Monroy,[74] S. Monteil,[9] M. Morandin,[28] G. Morello,[23] M. J. Morello,[29,p] J. Moron,[34] A. B. Morris,[75] A. G. Morris,[56] R. Mountain,[68] H. Mu,[3] F. Muheim,[58,48] M. Mulder,[48] D. Müller,[48] K. Müller,[50] C. H. Murphy,[63] D. Murray,[62] P. Muzzetto,[27,48] P. Naik,[54] T. Nakada,[49] R. Nandakumar,[57] T. Nanut,[49] I. Nasteva,[2] M. Needham,[58] I. Neri,[21] N. Neri,[25,q] S. Neubert,[75] N. Neufeld,[48] R. Newcombe,[61] T. D. Nguyen,[49] C. Nguyen-Mau,[49,t] E. M. Niel,[11] S. Nieswand,[14] N. Nikitin,[40] N. S. Nolte,[15] C. Nunez,[85] A. Oblakowska-Mucha,[34] V. Obraztsov,[44] D. P. O'Hanlon,[54] R. Oldeman,[27,g] M. E. Olivares,[68] C. J. G. Onderwater,[78] A. Ossowska,[35] J. M. Otalora Goicochea,[2] T. Ovsiannikova,[41] P. Owen,[50] A. Oyanguren,[47] B. Pagare,[56] P. R. Pais,[48] T. Pajero,[63] A. Palano,[19] M. Palutan,[23] Y. Pan,[62] G. Panshin,[83] A. Papanestis,[57] M. Pappagallo,[19,f] L. L. Pappalardo,[21,c] C. Pappenheimer,[65] W. Parker,[66] C. Parkes,[62] C. J. Parkinson,[46] B. Passalacqua,[21] G. Passaleva,[22] A. Pastore,[19] M. Patel,[61] C. Patrignani,[20,e] C. J. Pawley,[79] A. Pearce,[48] A. Pellegrino,[32] M. Pepe Altarelli,[48] S. Perazzini,[20] D. Pereima,[41] P. Perret,[9] M. Petric,[59,48] K. Petridis,[54] A. Petrolini,[24,a] A. Petrov,[80] S. Petrucci,[58] M. Petruzzo,[25] T. T. H. Pham,[68] A. Philippov,[42] L. Pica,[29,p] M. Piccini,[77] B. Pietrzyk,[8] G. Pietrzyk,[49] M. Pili,[63] D. Pinci,[30] F. Pisani,[48] Resmi P. K,[10] V. Placinta,[37] J. Plews,[53] M. Plo Casasus,[46] F. Polci,[13] M. Poli Lener,[23] M. Poliakova,[68] A. Poluektov,[10] N. Polukhina,[82,u] I. Polyakov,[68] E. Polycarpo,[2] G. J. Pomery,[54] S. Ponce,[48] D. Popov,[6,48] S. Popov,[42] S. Poslavskii,[44] K. Prasanth,[35] L. Promberger,[48] C. Prouve,[46] V. Pugatch,[52] H. Pullen,[63] G. Punzi,[29,v] W. Qian,[6] J. Qin,[6] R. Quagliani,[13] B. Quintana,[8] N. V. Raab,[18] R. I. Rabadan Trejo,[10] B. Rachwal,[34] J. H. Rademacker,[54] M. Rama,[29] M. Ramos Pernas,[56] M. S. Rangel,[2] F. Ratnikov,[42,81] G. Raven,[33] M. Reboud,[8] F. Redi,[49] F. Reiss,[62] C. Remon Alepuz,[47] Z. Ren,[3] V. Renaudin,[63] R. Ribatti,[29] S. Ricciardi,[57] K. Rinnert,[60] P. Robbe,[11] G. Robertson,[58] A. B. Rodrigues,[49] E. Rodrigues,[60] J. A. Rodriguez Lopez,[74] A. Rollings,[63] P. Roloff,[48] V. Romanovskiy,[44] M. Romero Lamas,[46] A. Romero Vidal,[46] J. D. Roth,[85] M. Rotondo,[23] M. S. Rudolph,[68] T. Ruf,[48] J. Ruiz Vidal,[47] A. Ryzhikov,[81] J. Ryzka,[34] J. J. Saborido Silva,[46] N. Sagidova,[38] N. Sahoo,[56] B. Saitta,[27,g] M. Salomoni,[48] C. Sanchez Gras,[32]

R. Santacesaria,[30] C. Santamarina Rios,[46] M. Santimaria,[23] E. Santovetti,[31,j] D. Saranin,[82] G. Sarpis,[14] M. Sarpis,[75] A. Sarti,[30] C. Satriano,[30,w] A. Satta,[31] M. Saur,[15] D. Savrina,[41,40] H. Sazak,[9] L. G. Scantlebury Smead,[63] S. Schael,[14] M. Schellenberg,[15] M. Schiller,[59] H. Schindler,[48] M. Schmelling,[16] B. Schmidt,[48] O. Schneider,[49] A. Schopper,[48] M. Schubiger,[32] S. Schulte,[49] M. H. Schune,[11] R. Schwemmer,[48] B. Sciascia,[23] S. Sellam,[46] A. Semennikov,[41] M. Senghi Soares,[33] A. Sergi,[24,a] N. Serra,[50] L. Sestini,[28] A. Seuthe,[15] P. Seyfert,[48] Y. Shang,[5] D. M. Shangase,[85] M. Shapkin,[44] I. Shchemerov,[82] L. Shchutska,[49] T. Shears,[60] L. Shekhtman,[43,h] Z. Shen,[5] V. Shevchenko,[80] E. B. Shields,[26,d] E. Shmanin,[82] J. D. Shupperd,[68] B. G. Siddi,[21] R. Silva Coutinho,[50] G. Simi,[28] S. Simone,[19,f] N. Skidmore,[62] T. Skwarnicki,[68] M. W. Slater,[53] I. Slazyk,[21,c] J. C. Smallwood,[63] J. G. Smeaton,[55] A. Smetkina,[41] E. Smith,[50] M. Smith,[61] A. Snoch,[32] M. Soares,[20] L. Soares Lavra,[9] M. D. Sokoloff,[65] F. J. P. Soler,[59] A. Solovev,[38] I. Solovyev,[38] F. L. Souza De Almeida,[2] B. Souza De Paula,[2] B. Spaan,[15] E. Spadaro Norella,[25,q] P. Spradlin,[59] F. Stagni,[48] M. Stahl,[65] S. Stahl,[48] P. Stefko,[49] O. Steinkamp,[50,82] O. Stenyakin,[44] H. Stevens,[15] S. Stone,[68] M. E. Stramaglia,[49] M. Straticiuc,[37] D. Strekalina,[82] F. Suljik,[63] J. Sun,[27] L. Sun,[73] Y. Sun,[66] P. Svihra,[62] P. N. Swallow,[53] K. Swientek,[34] A. Szabelski,[36] T. Szumlak,[34] M. Szymanski,[48] S. Taneja,[62] F. Teubert,[48] E. Thomas,[48] K. A. Thomson,[60] V. Tisserand,[9] S. T'Jampens,[8] M. Tobin,[4] L. Tomassetti,[21,c] D. Torres Machado,[1] D. Y. Tou,[13] M. T. Tran,[49] E. Trifonova,[82] C. Trippl,[49] G. Tuci,[29,v] A. Tully,[49] N. Tuning,[32,48] A. Ukleja,[36] D. J. Unverzagt,[17] E. Ursov,[82] A. Usachov,[32] A. Ustyuzhanin,[42,81] U. Uwer,[17] A. Vagner,[83] V. Vagnoni,[20] A. Valassi,[48] G. Valenti,[20] N. Valls Canudas,[84] M. van Beuzekom,[32] M. Van Dijk,[49] E. van Herwijnen,[82] C. B. Van Hulse,[18] M. van Veghel,[78] R. Vazquez Gomez,[46] P. Vazquez Regueiro,[46] C. Vázquez Sierra,[48] S. Vecchi,[21] J. J. Velthuis,[54] M. Veltri,[22,x] A. Venkateswaran,[68] M. Veronesi,[32] M. Vesterinen,[56] D. Vieira,[65] M. Vieites Diaz,[49] H. Viemann,[76] X. Vilasis-Cardona,[84] E. Vilella Figueras,[60] P. Vincent,[13] D. Vom Bruch,[10] A. Vorobyev,[38] V. Vorobyev,[43,h] N. Voropaev,[38] R. Waldi,[17] J. Walsh,[29] C. Wang,[17] J. Wang,[5] J. Wang,[4] J. Wang,[3] J. Wang,[73] M. Wang,[3] R. Wang,[54] Y. Wang,[7] Z. Wang,[50] Z. Wang,[3] H. M. Wark,[60] N. K. Watson,[53] S. G. Weber,[13] D. Websdale,[61] C. Weisser,[64] B. D. C. Westhenry,[54] D. J. White,[62] M. Whitehead,[54] D. Wiedner,[15] G. Wilkinson,[63] M. Wilkinson,[68] I. Williams,[55] M. Williams,[64] M. R. J. Williams,[58] F. F. Wilson,[57] W. Wislicki,[36] M. Witek,[35] L. Witola,[17] G. Wormser,[11] S. A. Wotton,[55] H. Wu,[68] K. Wyllie,[48] Z. Xiang,[6] D. Xiao,[7] Y. Xie,[7] A. Xu,[5] J. Xu,[6] L. Xu,[3] M. Xu,[7] Q. Xu,[6] Z. Xu,[5] Z. Xu,[6] D. Yang,[3] S. Yang,[6] Y. Yang,[6] Z. Yang,[3] Z. Yang,[66] Y. Yao,[68] L. E. Yeomans,[60] H. Yin,[7] J. Yu,[71] X. Yuan,[68] O. Yushchenko,[44] E. Zaffaroni,[49] M. Zavertyaev,[16,u] M. Zdybal,[35] O. Zenaiev,[48] M. Zeng,[3] D. Zhang,[7] L. Zhang,[3] S. Zhang,[5] Y. Zhang,[5] Y. Zhang,[63] A. Zhelezov,[17] Y. Zheng,[6] X. Zhou,[6] Y. Zhou,[6] X. Zhu,[3] Z. Zhu,[6] V. Zhukov,[14,40] J. B. Zonneveld,[58] Q. Zou,[4] S. Zucchelli,[20,e] D. Zuliani,[28] and G. Zunica[62]

(LHCb Collaboration)

[1]*Centro Brasileiro de Pesquisas Físicas (CBPF), Rio de Janeiro, Brazil*
[2]*Universidade Federal do Rio de Janeiro (UFRJ), Rio de Janeiro, Brazil*
[3]*Center for High Energy Physics, Tsinghua University, Beijing, China*
[4]*Institute Of High Energy Physics (IHEP), Beijing, China*
[5]*School of Physics State Key Laboratory of Nuclear Physics and Technology, Peking University, Beijing, China*
[6]*University of Chinese Academy of Sciences, Beijing, China*
[7]*Institute of Particle Physics, Central China Normal University, Wuhan, Hubei, China*
[8]*Université Savoie Mont Blanc, CNRS, IN2P3-LAPP, Annecy, France*
[9]*Université Clermont Auvergne, CNRS/IN2P3, LPC, Clermont-Ferrand, France*
[10]*Aix Marseille Université, CNRS/IN2P3, CPPM, Marseille, France*
[11]*Université Paris-Saclay, CNRS/IN2P3, IJCLab, Orsay, France*
[12]*Laboratoire Leprince-Ringuet, CNRS/IN2P3, Ecole Polytechnique, Institut Polytechnique de Paris, Palaiseau, France*
[13]*LPNHE, Sorbonne Université, Paris Diderot Sorbonne Paris Cité, CNRS/IN2P3, Paris, France*
[14]*I. Physikalisches Institut, RWTH Aachen University, Aachen, Germany*
[15]*Fakultät Physik, Technische Universität Dortmund, Dortmund, Germany*
[16]*Max-Planck-Institut für Kernphysik (MPIK), Heidelberg, Germany*
[17]*Physikalisches Institut, Ruprecht-Karls-Universität Heidelberg, Heidelberg, Germany*
[18]*School of Physics, University College Dublin, Dublin, Ireland*
[19]*INFN Sezione di Bari, Bari, Italy*
[20]*INFN Sezione di Bologna, Bologna, Italy*
[21]*INFN Sezione di Ferrara, Ferrara, Italy*
[22]*INFN Sezione di Firenze, Firenze, Italy*
[23]*INFN Laboratori Nazionali di Frascati, Frascati, Italy*
[24]*INFN Sezione di Genova, Genova, Italy*
[25]*INFN Sezione di Milano, Milano, Italy*
[26]*INFN Sezione di Milano-Bicocca, Milano, Italy*
[27]*INFN Sezione di Cagliari, Monserrato, Italy*
[28]*Universita degli Studi di Padova, Universita e INFN, Padova, Padova, Italy*

[29]*INFN Sezione di Pisa, Pisa, Italy*
[30]*INFN Sezione di Roma La Sapienza, Roma, Italy*
[31]*INFN Sezione di Roma Tor Vergata, Roma, Italy*
[32]*Nikhef National Institute for Subatomic Physics, Amsterdam, Netherlands*
[33]*Nikhef National Institute for Subatomic Physics and VU University Amsterdam, Amsterdam, Netherlands*
[34]*AGH - University of Science and Technology, Faculty of Physics and Applied Computer Science, Kraków, Poland*
[35]*Henryk Niewodniczanski Institute of Nuclear Physics Polish Academy of Sciences, Kraków, Poland*
[36]*National Center for Nuclear Research (NCBJ), Warsaw, Poland*
[37]*Horia Hulubei National Institute of Physics and Nuclear Engineering, Bucharest-Magurele, Romania*
[38]*Petersburg Nuclear Physics Institute NRC Kurchatov Institute (PNPI NRC KI), Gatchina, Russia*
[39]*Institute for Nuclear Research of the Russian Academy of Sciences (INR RAS), Moscow, Russia*
[40]*Institute of Nuclear Physics, Moscow State University (SINP MSU), Moscow, Russia*
[41]*Institute of Theoretical and Experimental Physics NRC Kurchatov Institute (ITEP NRC KI), Moscow, Russia*
[42]*Yandex School of Data Analysis, Moscow, Russia*
[43]*Budker Institute of Nuclear Physics (SB RAS), Novosibirsk, Russia*
[44]*Institute for High Energy Physics NRC Kurchatov Institute (IHEP NRC KI), Protvino, Russia, Protvino, Russia*
[45]*ICCUB, Universitat de Barcelona, Barcelona, Spain*
[46]*Instituto Galego de Física de Altas Enerxías (IGFAE), Universidade de Santiago de Compostela, Santiago de Compostela, Spain*
[47]*Instituto de Fisica Corpuscular, Centro Mixto Universidad de Valencia - CSIC, Valencia, Spain*
[48]*European Organization for Nuclear Research (CERN), Geneva, Switzerland*
[49]*Institute of Physics, Ecole Polytechnique Fédérale de Lausanne (EPFL), Lausanne, Switzerland*
[50]*Physik-Institut, Universität Zürich, Zürich, Switzerland*
[51]*NSC Kharkiv Institute of Physics and Technology (NSC KIPT), Kharkiv, Ukraine*
[52]*Institute for Nuclear Research of the National Academy of Sciences (KINR), Kyiv, Ukraine*
[53]*University of Birmingham, Birmingham, United Kingdom*
[54]*H. H. Wills Physics Laboratory, University of Bristol, Bristol, United Kingdom*
[55]*Cavendish Laboratory, University of Cambridge, Cambridge, United Kingdom*
[56]*Department of Physics, University of Warwick, Coventry, United Kingdom*
[57]*STFC Rutherford Appleton Laboratory, Didcot, United Kingdom*
[58]*School of Physics and Astronomy, University of Edinburgh, Edinburgh, United Kingdom*
[59]*School of Physics and Astronomy, University of Glasgow, Glasgow, United Kingdom*
[60]*Oliver Lodge Laboratory, University of Liverpool, Liverpool, United Kingdom*
[61]*Imperial College London, London, United Kingdom*
[62]*Department of Physics and Astronomy, University of Manchester, Manchester, United Kingdom*
[63]*Department of Physics, University of Oxford, Oxford, United Kingdom*
[64]*Massachusetts Institute of Technology, Cambridge, Massachusetts, USA*
[65]*University of Cincinnati, Cincinnati, Ohio, USA*
[66]*University of Maryland, College Park, Maryland, USA*
[67]*Los Alamos National Laboratory (LANL), Los Alamos, New Mexico, USA*
[68]*Syracuse University, Syracuse, New York, USA*
[69]*School of Physics and Astronomy, Monash University, Melbourne, Australia, associated to*[56]
[70]*Pontifícia Universidade Católica do Rio de Janeiro (PUC-Rio), Rio de Janeiro, Brazil, associated to*[2]
[71]*Physics and Micro Electronic College, Hunan University, Changsha City, China, associated to*[7]
[72]*Guangdong Provincial Key Laboratory of Nuclear Science, Guangdong-Hong Kong Joint Laboratory of Quantum Matter, Institute of Quantum Matter, South China Normal University, Guangzhou, China, associated to*[3]
[73]*School of Physics and Technology, Wuhan University, Wuhan, China, associated to*[3]
[74]*Departamento de Fisica, Universidad Nacional de Colombia, Bogota, Colombia, associated to*[13]
[75]*Universität Bonn - Helmholtz-Institut für Strahlen und Kernphysik, Bonn, Germany, associated to*[17]
[76]*Institut für Physik, Universität Rostock, Rostock, Germany, associated to*[17]
[77]*INFN Sezione di Perugia, Perugia, Italy, associated to*[21]
[78]*Van Swinderen Institute, University of Groningen, Groningen, Netherlands, associated to*[32]
[79]*Universiteit Maastricht, Maastricht, Netherlands, associated to*[32]
[80]*National Research Centre Kurchatov Institute, Moscow, Russia, associated to*[41]
[81]*National Research University Higher School of Economics, Moscow, Russia, associated to*[42]
[82]*National University of Science and Technology "MISIS", Moscow, Russia, associated to*[41]
[83]*National Research Tomsk Polytechnic University, Tomsk, Russia, associated to*[41]

[84] *DS4DS, La Salle, Universitat Ramon Llull, Barcelona, Spain, associated to*[45]
[85] *University of Michigan, Ann Arbor, Michigan, USA, associated to*[68]

[a] Also at Università di Genova, Genova, Italy.
[b] Also at Università di Modena e Reggio Emilia, Modena, Italy.
[c] Also at Università di Ferrara, Ferrara, Italy.
[d] Also at Università di Milano Bicocca, Milano, Italy.
[e] Also at Università di Bologna, Bologna, Italy.
[f] Also at Università di Bari, Bari, Italy.
[g] Also at Università di Cagliari, Cagliari, Italy.
[h] Also at Novosibirsk State University, Novosibirsk, Russia.
[i] Also at Department of Physics, Astronomy, Uppsala University, Uppsala, Sweden.
[j] Also at Università di Roma Tor Vergata, Roma, Italy.
[k] Also at Universidade Federal do Triângulo Mineiro (UFTM), Uberaba-MG, Brazil.
[l] Also at Hangzhou Institute for Advanced Study, UCAS, Hangzhou, China.
[m] Also at AGH - University of Science and Technology, Faculty of Computer Science, Electronics and Telecommunications, Kraków, Poland.
[n] Also at Università di Siena, Siena, Italy.
[o] Also at Università di Padova, Padova, Italy.
[p] Also at Scuola Normale Superiore, Pisa, Italy.
[q] Also at Università degli Studi di Milano, Milano, Italy.
[r] Also at MSU - Iligan Institute of Technology (MSU-IIT), Iligan, Philippines.
[s] Also at Università di Firenze, Firenze, Italy.
[t] Also at Hanoi University of Science, Hanoi, Vietnam.
[u] Also at P. N. Lebedev Physical Institute, Russian Academy of Science (LPI RAS), Moscow, Russia.
[v] Also at Università di Pisa, Pisa, Italy.
[w] Also at Università della Basilicata, Potenza, Italy.
[x] Also at Università di Urbino, Urbino, Italy.